

Calibration of Hole Scattering Rates in Silicon with a Large Set of Experimental Data including High Voltage Quantum Yield, Drain Disturb and Substrate Hole Injection

Andrea Ghetti
 ST Microelectronics, Central R&D
 20041 Agrate Brianza, Italy
 Email: andrea.ghetti@st.com

Abstract—In this paper we present an extensive calibration of hole scattering rates in silicon by comparing simulations with a large set of experimental data including high voltage quantum yield, and, for the first time, hole gate current during drain stress of non volatile memory cells, and substrate hot hole injection for both homogeneous injection (Ning’s experiment) and impact ionization feedback (hole CHISEL). The proposed model is compared to the models of [1], [2]. It is demonstrated that the inclusion of data sensitive to the high energy part of the hole distribution function points out that previously proposed models are not able to reproduce experimental data when very high fields are present, and allows to find more accurate scattering rates.

I. INTRODUCTION

With the continuous reduction of the physical dimensions of MOS transistors, high field hole transport is gaining more and more attention because of its interesting applications. For example, non local phenomena such as velocity overshoot can become important to improve pMOSFET performance. In addition, hot holes are involved in an impact ionization feedback (IIF, a.k.a. CHISEL) mechanism that can be exploited for low voltage programming of non volatile memory (NVM) cells [3]. Hot holes are also used to erase NROM cells [4]. Moreover, understanding hole transport is also important to address reliability issues since holes are believed to be responsible for oxide degradation and breakdown [5], [6].

One of the best suited techniques to investigate these phenomena is Monte Carlo (MC) simulation. Unfortunately, because of the uncertainties about model parameters, scattering rates (SR) must be calibrated by comparison with an appropriate set of experimental data. This has been done for electrons, and general consensus has already been reached about electron SR in silicon [7]. Table I shows the set of experiments that are typically used for calibration. Mobility/drift-velocity data probe the first few tens of eV of the distribution function (DF). Impact ionization coefficient and quantum yield (QY) are sensitive to the medium energies (1-3 eV), while homogeneous injection from the substrate (Ning’s experiment) probes the DF for energy near the top of the barrier (3.1eV for electrons, 4.7eV for holes).

TABLE I
EXPERIMENTAL DATA TYPICALLY USED FOR CALIBRATION

Experiment	Energy range	Electron	Hole	
		Available?	Available?	this work
Mobility drift-velocity	< 0.2 eV	Yes	Yes	
Imp. Ion. Coef.	1-3 eV	Yes	Yes	
Quantum Yield	1-3 eV	Yes	No	High volt. QY
Homogeneous injection	E_b	Yes	No/Few	hole IIF drain disturb

However, on the contrary of electrons, calibration of hole transport has received less attention so far, resulting in a large spread of published hole scattering rates. This is essentially because less experimental data were available for holes (cfr. Table I). Basically, only drift velocity and impact ionization coefficient, and more recently high voltage quantum yield, have been considered so far [1], [2], [8].

In this paper we present an extensive calibration of hole scattering rates in silicon by comparing simulations with an extended set of experimental data. Beside additional data of high voltage QY, we used impact ionization feedback data in pMOSFET and hole gate current (I_G) during drain stress on NVM cell as a probe of the high energy tail of the hole energy distribution (HDF). It is shown that the so-calibrated hole SR allow to reproduce a larger set of experimental conditions than previously published models, especially for very high fields.

This paper is arranged as follows. Section II outlines the main features of the MC simulator used in this work. Section III describes the calibration procedure and the obtained results. Practical applications of the proposed model are briefly illustrated in Sec. IV. Finally, Sec. V draws some conclusions.

II. MONTE CARLO MODELS

The adopted full band MC simulator (called FURBO) features the anisotropic silicon band structure which has been computed with the non local pseudopotential method. The irreducible wedge of the first Brillouin zone is discretized

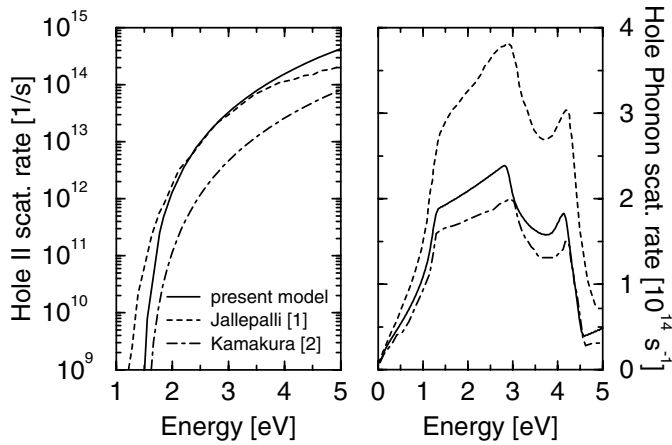


Fig. 1. Hole impact ionization and total phonon scattering rates investigated in this work. For the II scattering rate proposed here $P_0 = 8.5 \times 10^{12} \text{ s}^{-1} \text{ eV}^{-3.1}$ and $\gamma = 3.1$.

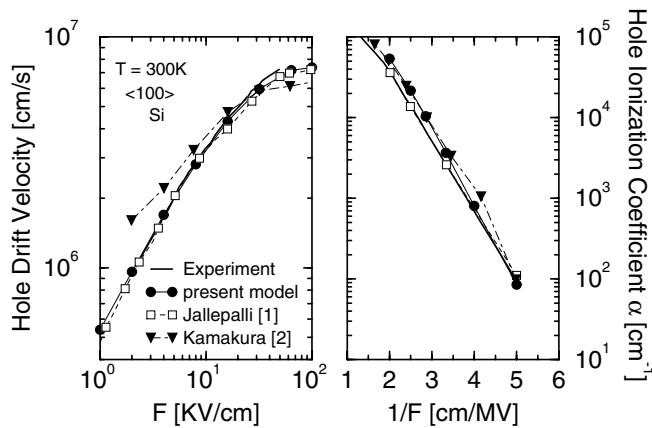


Fig. 2. Comparison of experimental (line) and simulated hole drift velocity (left) and II coefficient α (right). Experiments from [12] and [13].

with a regular cubic mesh featuring 80 elements along the X direction. The program is able to handle coupled silicon/oxide transport [9]. Electrons and holes can be simulated either simultaneously or through a sequence of steps as described in [10] that is needed for an accurate simulation of IIF.

Concerning hole transport, the valence band is described by 4 sub bands extending up to 12eV. Hole scattering mechanisms include elastic acoustic phonon, optical phonon and impact ionization (II). Hole II scattering rate is described by the relation $R_{II}(E) = P_0(E[eV] - 1.45[eV])^\gamma$ coming from full band calculation [11].

III. CALIBRATION RESULTS AND DISCUSSION

Parameters P_0 and γ , and phonon coupling constants were empirically adjusted until the best overall fit to a large set of experimental data was achieved, as demonstrated in the following. The so-calibrated SR are compared to the models of [1], [2] in Fig. 1.

Figure 2 shows that all these three models fit low energy experimental data although they provide very different HDF (Fig. 3). In particular, the II coefficient is the same because the reduced hole population at high energy is compensated

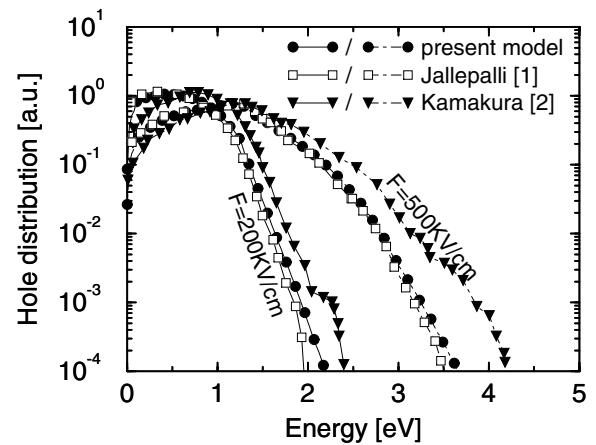


Fig. 3. Comparison of hole distribution function in homogeneous field provided by the three investigated models.

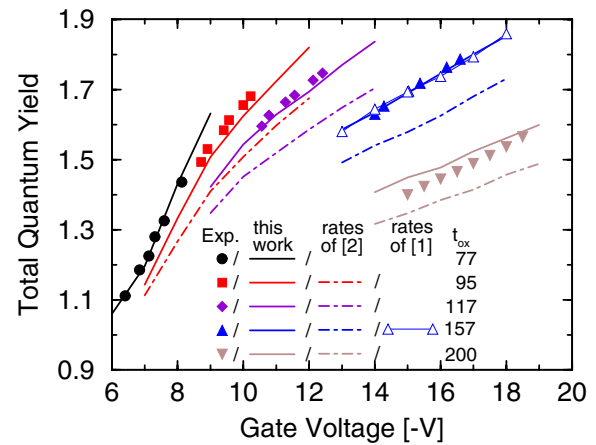


Fig. 4. Comparison of experimental (filled symbols) and simulated (lines and open symbols) high voltage Quantum Yield. Experimental data from [2].

by the higher II scattering rate. However, the three models would provides very different results when quantities sensitive only to the number of hot holes, such as I_G , are considered. That is why, in order to discriminate among them, other experimental conditions must be considered. To this purpose, we will compare in the following simulation results provided by our code with the adoption of all the three scattering models of Fig. 1.

Figure 4 shows high voltage QY results. In this experiment, electrons are injected with a high energy, because of the high (negative) gate voltage, in the substrate of a pMOSFET where they create new electron-hole pair by II. The ratio of the generated holes and the injected electrons is the QY. If the gate voltage is high enough, secondary holes have enough energy to ionize again contributing to the total number of generated pairs. Since the electron contribution is quantitatively reproduced by our simulator [9], [14], Fig. 4 points out the difference due only to hole SR. As it is possible to see, SR of [2] sensibly underestimates experimental data, while the proposed SR and those of [1] are in good agreement with the experiments.

Next, hot hole I_G data, that are sensitive to holes with

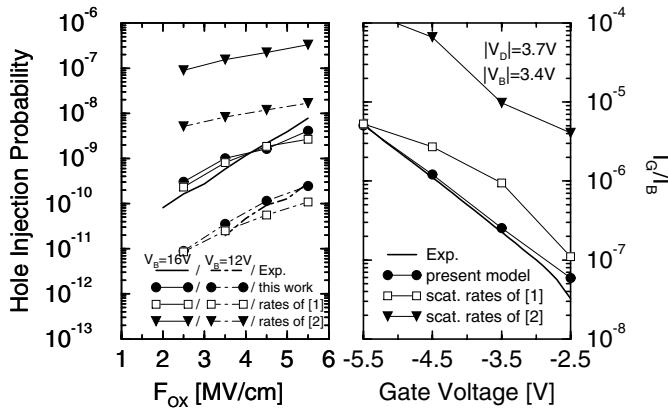


Fig. 5. Comparison of experimental substrate hole injection (line) and simulation (symbols). Left: homogeneous injection (Ning's experiment). Measurements from [15]. Right: impact ionization feedback (hole CHISEL). Experiments from [16].

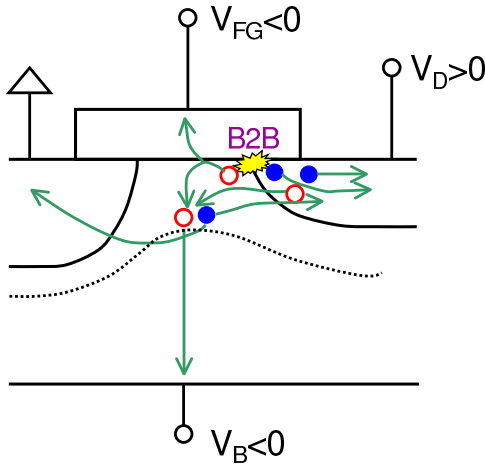


Fig. 6. Schematic representation of the drain disturb regime.

energy around the Si/SiO₂ valence band barrier ($E_b \approx 4.7$ eV), will be considered. Substrate homogeneous injection results are shown in Fig. 5.left. In this experiment, holes are generated at the edge of the substrate depletion region, and then accelerated toward the interface where some of them have enough energy to be injected over the barrier. The ratio of injected holes and those impinging on the interface is the injection probability (P_{inj}) shown in Fig. 5.left. SR of [2] largely overestimates experimental data, pointing out that both phonon and II SR of [2] are too low. Similar conclusion can be drawn by looking at the comparison about substrate enhanced hot hole I_G [16] (i.e. the CHISEL mechanism [17] but for holes) shown in Fig. 5.right. However, in this latter case, it is also possible to appreciate a difference between the proposed SR and those of [1] because of the higher fields attained in this device due to the higher substrate doping. This difference is attributed to the higher II SR of the present model for energy $> 4eV$ (see Fig. 1) that effectively reduces HDF for such high energy.

Finally, we calibrated hole SR also against hot hole I_G in drain disturb configuration of NVM that is schematically

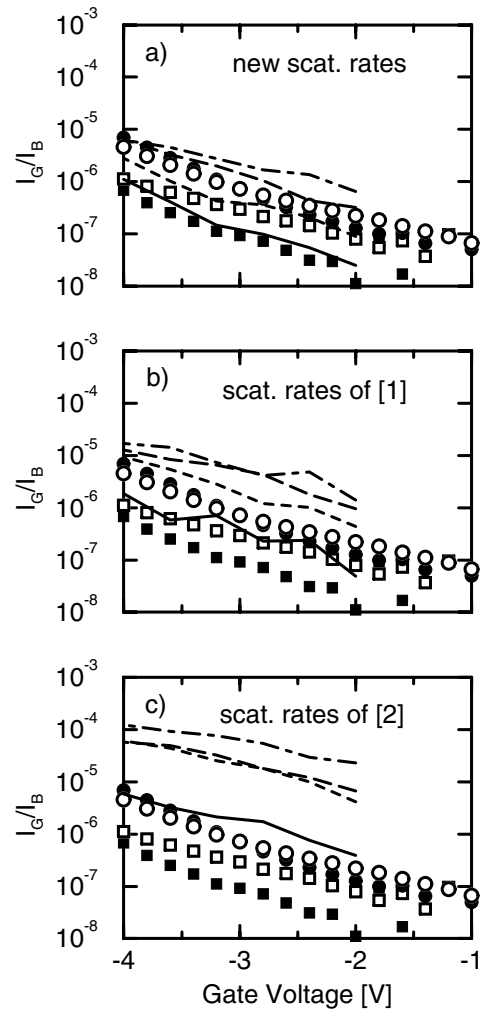


Fig. 7. Comparison of experimental normalized hole gate current I_G/I_B (symbols) with simulations (lines) adopting different scattering rates. $V_G = -4V$, $t_{ox} = 7nm$ and solid line/■: $V_D = 4.2V$, $V_B = 0V$; dashed line/□: $V_D = 4.2V$, $V_B = -1.6V$; long-dashed line/●: $V_D = 5V$, $V_B = 0V$; dot-dashed line/o: $V_D = 5V$, $V_B = -1.2V$. a) proposed scattering rates. b) scattering rates of [1]. c) scattering rates of [2].

depicted in Fig. 6. In retention, floating gate voltage is negative because of the negative charge stored in it, while drain voltage can be high if the cell belongs to the same bit line of another cell that is being programmed. In this condition, holes (h1) are generated by band to band tunneling at the interface near the drain junction. The electric field pushes these holes first against the interface, and then toward the substrate contact. Along this trajectory holes are heated up by the strong interface field due the high drain-to-bulk (V_{DB}) potential and the negative gate voltage that partially depletes the drain. Therefore holes can be injected in the gate (partially erasing the cell) or generate electrons (e2) by II. While traveling toward the drain these electrons gain energy at the expense V_{DB} generating additional holes (h3) by II in the high field region of the drain. These tertiary holes are again accelerated toward the interface, and so on. Figures 7, 8 compare simulations and experimental data of hole I_G in drain

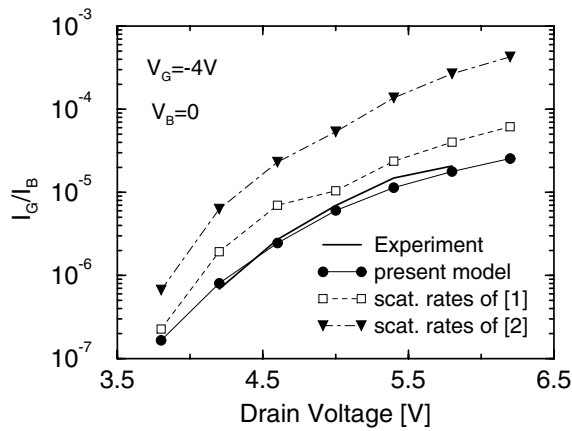


Fig. 8. Hole I_G as a function of the drain voltage for the same device of Fig. 7.

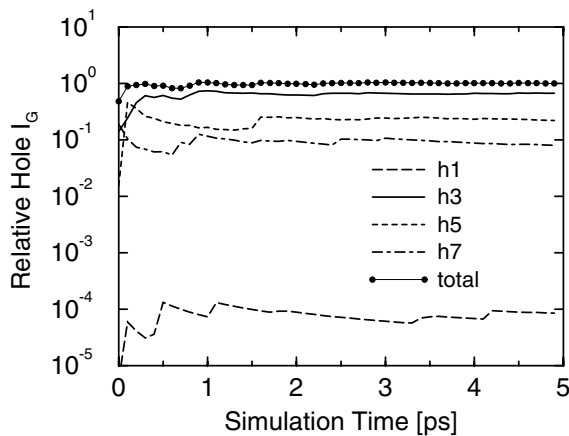


Fig. 9. Contribution of the different hole components to I_G normalized to the final value of the total current for $V_G = -4V$, $V_D = 4.2V$, $V_B = 0V$.

disturb configuration. This device features an oxide thickness of 7nm, that is much smaller than standard NVM product and that has been chosen to emphasize the phenomenon. Even this case points out the differences among the three considered models, indicating that the present model better reproduces hot hole I_G bias dependence.

IV. APPLICATIONS

The hole SR calibrated in this work have been then used for a detailed investigation of the drain disturb problem in NVM. For example, Fig. 9 shows the relative contribution of the different hole component to I_G . The largest contribution (about 67% for the bias point of Fig. 9) comes from the tertiary holes (h3) because they are hotter than primary holes generated by band-to-band tunneling (h1) since they, differently from h1, are generated with some energy and see a higher voltage drop of a band gap. This result points out the necessity to include also electrons in this kind of simulation.

Next, we investigated the voltage dependence of the drain disturb. In first approximation, we can assume that the programming speed depends on V_{DB} . Therefore, for a given V_{DB} (i.e. programming speed) it is of interest to study how to divide the total V_{DB} between drain and body in order to minimize the

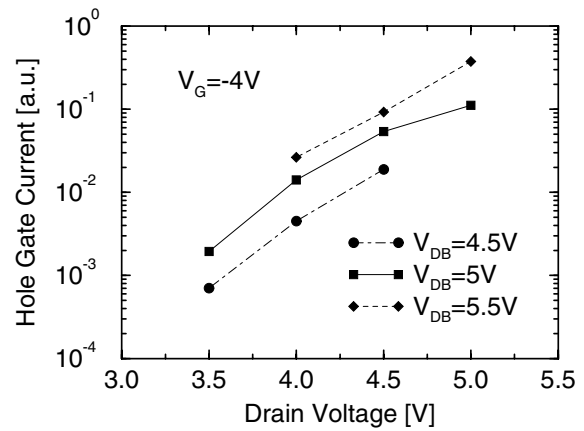


Fig. 10. Simulated drain voltage dependence of the hole gate current for constant drain-to-bulk (V_{DB}) voltage.

hole I_G that is responsible for oxide degradation. This is done in Fig. 10. Reducing the drain voltage (V_D) while increasing the bulk voltage (V_B) to keep the same V_{DB} results in a smaller hole I_G , and thus in less degradation. These results suggest the beneficial effect on drain disturb of a reduced V_D /increased V_B for the same programming speed.

V. CONCLUSION

In summary, we have calibrated hole scattering rates in silicon to reproduce a large set of experimental data. The proposed model reproduces hot hole phenomena better than previously published models. Therefore it is of particular interest to investigate hot hole related issues such as velocity overshoot and substrate current in pMOSFET, oxide degradation and reliability, drain disturb in NVM cells, and erasing of NROM like NVM.

ACKNOWLEDGMENT

The author would like to thank Silvia Beltrami and Mauro Bonanomi for providing the experimental data about drain disturb.

REFERENCES

- [1] S. Jallepalli *et al.*, *Jour. Appl. Phys.*, vol. 81, no. 5, p. 2250, 1997.
- [2] Y. Kamakura *et al.*, *Jour. Appl. Phys.*, vol. 88, no. 10, p. 5802, 2000.
- [3] J. D. Bude *et al.*, in *IEDM Technical Digest*, p. 989, 1995.
- [4] B. Eitan *et al.*, *IEEE Electron Device Lett.*, vol. 21, no. 11, p. 543, 2000.
- [5] K. Schuegraf *et al.*, *IEEE Trans. Electron Devices*, vol. 41, no. 5, p. 761, 1994.
- [6] J. Bude *et al.*, in *IEDM Technical Digest*, p. 179, 1998.
- [7] M. Fischetti *et al.*, in *Proc. ESSDERC Conf.*, p. 813, 1996.
- [8] M. Fischetti *et al.*, *IEEE on line TCAD Journal*, <http://www.ieee.org/products/online/journal/accepted/fischetti-feb97/>, no. 3, 1997.
- [9] A. Ghetti, in *Proc. SISPAD Conference*, p. 231, 2002.
- [10] D. Esseni *et al.*, *IEEE Trans. Electron Devices*, vol. 47, no. 11, p. 2194, 2000.
- [11] T. Kunikiyo *et al.*, *Jour. Appl. Phys.*, vol. 79, no. 10, p. 7718, 1996.
- [12] G. Ottaviani *et al.*, *Phys. Rev. B*, vol. 12, p. 3318, 1975.
- [13] W. N. Grant, *Solid-State Electronics*, vol. 16, p. 1189, 1973.
- [14] A. Ghetti *et al.*, *IEEE Trans. Electron Devices*, vol. 47, no. 7, p. 1341, 2000.
- [15] L. Selmi *et al.*, in *IEDM Technical Digest*, p. 333, Dec. 1993.
- [16] F. Driussi *et al.*, in *Proc. ESSDERC Conf.*, p. 136, 2000.
- [17] J. D. Bude, in *Proc. Symp. on VLSI Technology*, p. 101, 1995.